

Antibody Responses during Hepatitis B Viral Infection

Stanca M. Ciupe^{1*}, Ruy M. Ribeiro², Alan S. Perelson²

1 Department of Mathematics, Virginia Tech, Blacksburg, Virginia, United States of America, **2** Theoretical Division, Los Alamos National Laboratory, Los Alamos, New Mexico, United States of America



Abstract

Hepatitis B is a DNA virus that infects liver cells and can cause both acute and chronic disease. It is believed that both viral and host factors are responsible for determining whether the infection is cleared or becomes chronic. Here we investigate the mechanism of protection by developing a mathematical model of the antibody response following hepatitis B virus (HBV) infection. We fitted the model to data from seven infected adults identified during acute infection and determined the ability of the virus to escape neutralization through overproduction of non-infectious subviral particles, which have HBs proteins on their surface, but do not contain nucleocapsid protein and viral nucleic acids. We showed that viral clearance can be achieved for high anti-HBV antibody levels, as in vaccinated individuals, when: (1) the rate of synthesis of hepatitis B subviral particles is slow; (2) the rate of synthesis of hepatitis B subviral particles is high but either anti-HBV antibody production is fast, the antibody affinity is high, or the levels of pre-existent HBV-specific antibody at the time of infection are high, as could be attained by vaccination. We further showed that viral clearance can be achieved for low equilibrium anti-HBV antibody levels, as in unvaccinated individuals, when a strong cellular immune response controls early infection.

Citation: Ciupe SM, Ribeiro RM, Perelson AS (2014) Antibody Responses during Hepatitis B Viral Infection. *PLoS Comput Biol* 10(7): e1003730. doi:10.1371/journal.pcbi.1003730

Editor: Roland R. Regoes, ETH Zurich, Switzerland

Received: October 11, 2013; **Accepted:** May 16, 2014; **Published:** July 31, 2014

This is an open-access article, free of all copyright, and may be freely reproduced, distributed, transmitted, modified, built upon, or otherwise used by anyone for any lawful purpose. The work is made available under the Creative Commons CC0 public domain dedication.

Funding: SMC acknowledges support from NSF grant DMS-1214582. Portions of this work were performed under the auspices of the U.S. Department of Energy under contract DE-AC52-06NA25396 and supported by NIH grants P20-GM103452, A1028433 and OD011095. The funders had no role in study design, data collection and analysis, decision to publish, or preparation of the manuscript.

Competing Interests: The authors have declared that no competing interests exist.

* Email: stanca@math.vt.edu

Introduction

Infection with hepatitis B virus (HBV) results in acute hepatitis followed by recovery in 85%–95% of human adults [1]. Recovery occurs when the organism mounts adequate immune responses against the virus. Such responses include production of protective, neutralizing antibodies against HBV surface antigen (HBsAg) [2,3], activation of strong and diversified CD4 and CD8 T-cells [4,2], expression of antiviral cytokines in the liver, such as gamma interferon and tumor necrosis factor alpha [5,6,7,8], and generation of cells that are protected from reinfection [9,10]. In contrast, progression to chronic HBV infection occurs predominantly in immuno-compromised adults and in unvaccinated infants [11]. Such individuals exhibit weak and inefficient humoral and cellular immune responses, resulting in continual virus replication and HBV surface antigenemia [12,4]. Little is known about the relative contributions of different arms of the immune system, especially the roles of neutralizing antibodies in the onset and outcome of infection.

The antibody response to HBV infection is difficult to study experimentally. Free antibody to surface antigen is not detected until after the resolution of HBV infection [13]. However, circulating immune complexes containing antibody and HBsAg are found in both acute and chronic HBV infections, suggesting that antibodies are produced much sooner than detected, and that they might play a role in the pathology of the disease [14,15,16,17]. HBsAg-specific antibodies have neutralizing properties and mediate protective immunity [16].

Infection with hepatitis B virus results in the synthesis of a large number, probably of at least 1,000-fold, of “subviral particles”

(SVPs) in relation to HBV particles [1,18]. SVPs, which are produced by HBV infected cells, are particles that have HBV proteins on their surface, but do not contain nucleocapsid protein and viral nucleic acids and hence are non-infectious [19]. They exist in two main forms: spheres 25 nm in diameter and filaments 22 nm in diameter with variable lengths [20,21,22,23]. The reasons for their overproduction and their contribution to HBV pathogenesis is still under investigation [24]. SVPs may influence the way the host reacts to HBV infection. They may induce tolerance during perinatal infection, thus delaying the rise of neutralizing antibodies. Additionally, the excess of subviral particles can serve as a decoy by adsorbing neutralizing antibodies and therefore delay the clearance of infection.

In this paper, we aim to determine quantitative features of the antibody responses to virus and subviral particles following HBV infection. We build on basic chronic virus infection models [25,26,27,28,29,30,31] and determine the antibody characteristics that explain both the high peak and eventual viral clearance observed during acute hepatitis B infections [8]. We show that antibody responses can lead to viral clearance when the anti-HBV levels are high, as in vaccinated patients, and: (1) the rate of synthesis of hepatitis B subviral particles is slow; (2) the rate of synthesis of hepatitis B subviral particles is high but either anti-HBV antibody production is fast, the antibodies have high affinity, or the levels of pre-existent HBV-specific antibody at the time of infection are high. For lower anti-HBV antibody levels, as in unvaccinated patients, both cellular and humoral responses are needed in concert to clear acute HBV infection with the CD8 T cells controlling the initial burst of replication and the antibodies preventing virus rebound. The paper is structured as follows. In section Methods we develop

Author Summary

Hepatitis B vaccine induces life-long protection in vaccinated individuals. In the absence of vaccination, however, hepatitis B virus can cause both self-limiting and chronic disease. We investigate whether antibodies against hepatitis B play a role in virus clearance. We developed a mathematical model that describes the production of antibodies to both infectious virus and non-infectious subviral particles (with hepatitis B surface proteins, but no nucleic acids) and compared the model to patient data. We predict that high levels of antibodies, either pre-existing, as in vaccinated individuals, or through fast expansion, can control the infection and lead to viral clearance. However, when the antibody levels are more similar to those observed in a clinical context, cellular immune responses are needed to control the virus and antibodies act only in late stages to aid in viral clearance.

the general model of antibody responses to viral and the subviral particles. In section Analytical results we analyze it analytically using asymptotic analysis techniques and in section Numerical results we present numerical results and compare these to data of primary HBV infection in humans, and present alternative models. We conclude with a discussion.

Methods

Models of virus infection in the absence of antibody responses

Standard mathematical models of viral infections consider dynamics and relations among uninfected target cells (T), infected cells (I), and virus (V) [25,26,27,28,29]. Briefly, these models assume that target cells T become infected at a rate proportional to both the target cell concentration and the virus concentration, *i.e.*, at rate βTV . Infected cells are thus produced at rate βTV and die at rate δ (that includes immune system mediated killing). Virus is produced by infected cells at rate π and is cleared at rate c . These models have been adapted to describe hepatitis B virus infection where the target population is liver cells (hepatocytes) [30,25,31]. The model accounts for the liver's ability to regenerate following injury [32,33]. This regeneration, accomplished by several cycles of hepatocyte mitosis, is described by a logistic term with carrying capacity T_m and maximal proliferation rate r [9,34]. Moreover, infected hepatocytes can be cured [10] and move back into the target population at rate ρ [30,31]. The dynamics of the system are governed by the following equations

$$\begin{aligned}\frac{dT}{dt} &= rT\left(1 - \frac{T+I}{T_m}\right) - \beta VT + \rho I, \\ \frac{dI}{dt} &= \beta VT - \delta I - \rho I, \\ \frac{dV}{dt} &= \pi I - cV,\end{aligned}\quad (1)$$

where for acute infection $T(0) = T_m > 0$, $I(0) = 0$ and $V(0) = V_0 > 0$. An analysis of this system predicts two outcomes [35,36,37]. The infection dies out when

$$R_0 = \frac{\pi\beta T_m}{c(\delta + \rho)} < 1$$

and the infection takes off and leads to chronic hepatitis when

$$R_0 = \frac{\pi\beta T_m}{c(\delta + \rho)} > 1.$$

This simple system, which lacks any explicit immune response, does not explain transient infections, where the liver gets infected, *i.e.*, $R_0 > 1$, but the infection is eventually cleared, presumably by the immune system. Clearance of HBV infection occurs in 90% of adults infected with HBV [1]. While the role of the cellular immune responses has been studied both theoretically and experimentally [9,34,38,39], less is known about the dynamics of the humoral immune response to HBV [40]. In the following section we investigate antibody responses by modifying system (1) to account for humoral immunity following HBV infection.

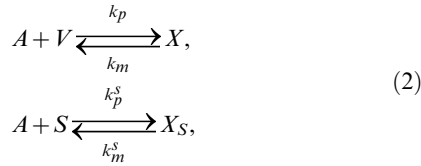
A model of HBV infection including an antibody response

To include the antibody response, we generalize the model given by Eq. (1) by considering seven populations, corresponding to target cells (T), which are mostly or exclusively uninfected hepatocytes, productively infected cells (I), free virus (V), free subviral particles (S), free antibody (A), virus-antibody complexes (X), and subviral particle-antibody complexes (X_S). Since hepatocytes are in contact with the blood we assume, as above, that their infection can be described by a well-mixed system. Further investigation is needed to know whether spatial effects are important in HBV infection. For hepatitis C virus (HCV) infection, in which a much smaller fraction of cells become infected, spatial clustering of infected cells has recently been observed [41].

As in Eq. (1), we assumed that target cells are maintained through homeostasis described by the logistic term with carrying capacity T_m and maximum proliferation rate r , and become infected at a rate proportional to both the target cell concentration and the virus concentration, *i.e.*, at rate βTV . Infected cells are thus produced at rate βTV and die at rate δ (that includes immune system mediated killing). Upon infection, virus and subviral particles are produced at rates π and $\pi\theta$, and cleared at rates c and c_s , respectively. We neglect the curing of infected cells by setting $\rho = 0$. With this simplification the basic reproductive number becomes $R_0 = \frac{\pi\beta T_m}{c\delta}$.

Previous papers [42,43] have presented detailed models of B lymphocyte proliferation and differentiation into plasmablast, antibody producing plasma cells and memory cells after they encounter antigen. For simplicity, we ignore the details of B-lymphocyte dynamics and differentiation into antibody producing cells and assume that free antibody (A), is produced at rate p_A proportional to the antigen load, *i.e.*, the viral and subviral concentrations, and is degraded at rate d_A . Antibody is maintained after virus is cleared through antigen-independent homeostatic proliferation of memory B cells and long-lived plasma cells. In order to model this in a simple way, we add a logistic term to the antibody equation with maximum proliferation rate r_A and carrying capacity A_m . We show (in section 4.3) that a model that explicitly includes B cell dynamics has behavior similar to this simpler model with antibody alone.

Antigen elimination is facilitated by the formation of antigen-antibody complexes. We consider the reversible binding of free anti-HBsAg antibody (A), to both free virus (V), and subviral particles (S), described by the reaction scheme



where X and X_S are the complexes formed between antibody and the viral and subviral particles, respectively. k_p, k_p^s are binding rate constants, and k_m, k_m^s are disassociation rate constants for antibody reacting to viral and subviral particles, respectively. We consider that complexes X and X_S are degraded at a constant rates c_{AV} and c_{AS} . Antibodies can also bind infected cells budding virus. In this model we consider this to occur at a small rate and we neglect it.

Based on the scheme (2) and the assumptions above we construct the following equations of virus-host interaction

$$\begin{aligned}
 \frac{dT}{dt} &= rT(1 - \frac{T+I}{T_m}) - \beta VT, \\
 \frac{dI}{dt} &= \beta VT - \delta I, \\
 \frac{dA}{dt} &= p_A(V+S) + r_{AA}(1 - \frac{A}{A_m}) + \\
 &k_m X - k_p AV + k_m^s X_S - k_p^s AS - d_{AA} A, \\
 \frac{dX}{dt} &= -k_m X + k_p AV - c_{AV} X, \\
 \frac{dX_S}{dt} &= -k_m^s X_S + k_p^s AS - c_{AS} X_S, \\
 \frac{dV}{dt} &= \pi I - cV + k_m X - k_p AV, \\
 \frac{dS}{dt} &= \pi \theta I - c_S S + k_m^s X_S - k_p^s AS,
 \end{aligned} \tag{3}$$

where $T(0) = T_m > 0$, $I(0) = 0$, $A(0) = 0$, $V(0) = V_0 > 0$, $S(0) = 0$, $X(0) = 0$ and $X_S(0) = 0$. The total concentration of viral DNA is described by

$$V_T = V + X, \tag{4}$$

and the total concentration of anti-HBsAg antibody is given by

$$A_T = A + X + X_S. \tag{5}$$

Results

Analytical results

Quasi-equilibrium of subviral particles. Not much is known about the differences in antibody response to viral and subviral particles. Therefore, for simplicity and to gain analytical insights into the model's behavior, we assume that the antibody association and disassociation rates and clearance rates are equal for the viral and subviral particles and virus-antibody and subviral particle-antibody complexes, *i.e.* $k_m = k_m^s$, $k_p = k_p^s$, $c = c_S$ and $c_{AV} = c_{AS}$. In section 4, we relax these simplifying assumptions. From the equilibrium of the X and X_S equations, we obtain that $\frac{V}{S} = \frac{X}{X_S}$. Similarly, at equilibrium

$$\begin{aligned}
 \frac{dV}{dt} + \frac{dX}{dt} &= 0 \Rightarrow \pi I = cV + c_{AV} X = \\
 c \frac{SX}{X_S} + c_{AV} X &= \frac{X}{X_S} (cS + c_{AV} X_S) \quad \text{and} \\
 \frac{dS}{dt} + \frac{dX_S}{dt} &= 0 \Rightarrow \pi I = \frac{1}{\theta} (cS + c_{AV} X_S),
 \end{aligned} \tag{6}$$

from which it follows that, at equilibrium the concentration of subviral particles (free and bound) is proportional to the concentration of the virus (free and bound), *i.e.* $S = \theta V$ and $X_S = \theta X$. Assuming quasi-steady state between the subviral particles and the free virus, we can incorporate these proportionalities into the system given by (3), reducing it to

$$\begin{aligned}
 \frac{dT}{dt} &= rT(1 - \frac{T+I}{T_m}) - \beta VT, \\
 \frac{dI}{dt} &= \beta VT - \delta I, \\
 \frac{dA}{dt} &= p_A(1 + \theta)V + r_{AA}(1 - \frac{A}{A_m}) + \\
 &(1 + \theta)k_m X - (1 + \theta)k_p AV - d_{AA} A, \\
 \frac{dX}{dt} &= -k_m X + k_p AV - c_{AV} X, \\
 \frac{dV}{dt} &= \pi I - cV + k_m X - k_p AV,
 \end{aligned} \tag{7}$$

where $T(0) = T_m > 0$, $I(0) = 0$, $A(0) = 0$, $V(0) = V_0 > 0$ and $X(0) = 0$. The $1 + \theta$ terms are included to account for the antibody binding to SVPs. We will refer to system (7) as the antibody model.

Asymptotic analysis. We rewrite the terms on the right hand side of system (7) describing antibody dynamics in the absence of virus as follows:

$$r_{AA}A(1 - \frac{A}{A_m}) - d_{AA}A = \rho_A A(1 - \frac{A}{\Gamma}), \tag{8}$$

where $\rho_A = r_{AA} - d_{AA}$ and $\Gamma = A_m(1 - d_{AA}/r_{AA})$ and study the long term behavior of system (7).

We distinguish between different scenarios of hepatitis B infection outcome (failure, exposure without establishment of infection, cleared and chronic infections) based on the relative parameter values. The system has the following non-negative steady states

- Infection cleared with liver failure in the absence of immune response

$$S_1 = (\bar{T}_1, \bar{I}_1, \bar{A}_1, \bar{X}_1, \bar{V}_1) = (0, 0, 0, 0, 0). \tag{9}$$

- Infection cleared with liver failure in the presence of immune response

$$S_2 = (\bar{T}_2, \bar{I}_2, \bar{A}_2, \bar{X}_2, \bar{V}_2) = (0, 0, \Gamma, 0, 0). \tag{10}$$

c. No-infection steady state

$$S_3 = (\bar{T}_3, \bar{I}_3, \bar{A}_3, \bar{X}_3, \bar{V}_3) = (T_m, 0, 0, 0, 0). \quad (11)$$

d. Cleared infection steady state, in the presence of an immune response

$$S_4 = (\bar{T}_4, \bar{I}_4, \bar{A}_4, \bar{X}_4, \bar{V}_4) = (T_m, 0, \Gamma, 0, 0). \quad (12)$$

e. Chronic infection steady states

$$S_5 = (\bar{T}_5, \bar{I}_5, \bar{A}_5, \bar{X}_5, \bar{V}_5). \quad (13)$$

with

$$\begin{aligned} a_1 \bar{A}_5^3 + a_2 \bar{A}_5^2 + a_3 \bar{A}_5 + a_4 &= 0, \\ \bar{T}_5 &= \frac{\delta}{\beta\pi} (c + \xi \bar{A}_5), \\ \bar{V}_5 &= \frac{\rho_A \bar{A}_5 (1 - \frac{\bar{A}_5}{\Gamma})}{(1 + \theta)(\xi \bar{A}_5 - p_A)} = \frac{r(1 - \frac{1}{R_0}(1 + \frac{\xi}{c} \bar{A}_5))}{\beta + \frac{r}{\pi T_m}(c + \xi \bar{A}_5)}, \quad (14) \\ \bar{I}_5 &= \frac{(c + \xi \bar{A}_5) \bar{V}_5}{\pi}, \\ \bar{X}_5 &= \frac{\xi}{c_{AV}} \bar{A}_5 \bar{V}_5, \end{aligned}$$

where

$$\begin{aligned} \xi &= \frac{c_{AV} k_p}{c_{AV} + k_m}, \\ a_1 &= r \rho_A \beta \xi, \\ a_2 &= \rho_A \beta (\pi \beta T_m + rc) - r \Gamma \xi (\rho_A \beta + \delta \xi (1 + \theta)), \quad (15) \\ a_3 &= r \Gamma \xi c \delta (R_0 - 1) (1 + \theta) + \\ &\Gamma (r \delta p_A \xi (1 + \theta) - \beta \rho_A (\pi \beta T_m + rc)), \\ a_4 &= r \Gamma p_A c \delta (1 + \theta) (1 - R_0). \end{aligned}$$

When $R_0 > 1$ we have that $a_4 < 0$. Therefore, since $a_1 > 0$, by Descartes' rule of signs, the polynomial in Eq. (14) can have one or three positive roots. Since we require positivity for \bar{V}_5 , $r(1 - \frac{1}{R_0}(1 + \frac{\xi}{c} \bar{A}_5)) > 0$, which is equivalent to

$$R_0 > 1 + \frac{\xi}{c} \bar{A}_5, \quad (16)$$

and to expression $\frac{\rho_A \bar{A}_5 (1 - \frac{\bar{A}_5}{\Gamma})}{(1 + \theta)(\xi \bar{A}_5 - p_A)} > 0$, which is satisfied when

$$\min\{\Gamma, \frac{p_A}{\xi}\} < \bar{A}_5 < \max\{\Gamma, \frac{p_A}{\xi}\}. \quad (17)$$

We cannot give definite conditions for when three roots emerge.

For each of the steady state solutions, S_1 to S_5 , we can analyze the local stability by studying the Jacobian matrix

$$J = \begin{pmatrix} r(1 - \frac{2\bar{T}_m}{T_m}) - \beta V - \lambda & -r \frac{\bar{T}_m}{T_m} & 0 & 0 & -\beta T \\ \beta V & -\delta - \lambda & 0 & 0 & \beta T \\ 0 & 0 & \rho_A(1 - \frac{2\bar{A}}{A}) - (1 + \theta)k_p V - \lambda & (1 + \theta)k_m & (1 + \theta)(p_A - k_p A) \\ 0 & 0 & k_p V & -k_m - c_{AV} - \lambda & k_p A \\ 0 & \pi & -k_p V & k_m & -c - k_p A - \lambda \end{pmatrix}. \quad (18)$$

Proposition 1. *The liver failure steady states S_1 and S_2 are always unstable.*

Proposition 2. *The no-infection steady state S_3 is always unstable.*

Proposition 3. *The cleared infection steady state S_4 is locally asymptotically stable when*

$$R_0 < 1 + \frac{\xi}{c} \Gamma, \quad (19)$$

and unstable otherwise.

Proof. The characteristic equation is given by

$$(\lambda + r)(\lambda + \rho_A)(\lambda^3 + b_1 \lambda^2 + b_2 \lambda + b_3) = 0, \quad (20)$$

where

$$\begin{aligned} b_1 &= c + \delta + k_p \Gamma + k_m + c_{AV}, \\ b_2 &= (c_{AV} + k_m)(c + \delta) + c \delta (1 - R_0) + (\delta + c_{AV}) k_p \Gamma, \quad (21) \\ b_3 &= (c_{AV} + k_m) c \delta (1 - R_0) + \delta c_{AV} k_p \Gamma. \end{aligned}$$

By Routh-Hurwitz conditions S_4 is locally asymptotically stable when $b_1 > 0$, $b_3 > 0$, and $b_1 b_2 - b_3 > 0$. This happens when condition (19) holds. Conversely, when (19) fails S_4 is unstable.

Finding explicit parameter values for the existence of chronic steady states and studying their stability is possible, but tedious and will not be presented here.

If $R_0 > 1 + \frac{\xi}{c} \Gamma$ clearance cannot be attained. Instead either a locally asymptotically stable chronic steady state or a limit cycle emerges regardless of θ , as we will illustrate numerically. If $R_0 < 1 + \frac{\xi}{c} \Gamma$ and $\bar{A}_5 > \Gamma$ then, from (16) and (17), the chronic steady state S_5 does not exist. Numerical results show that S_4 , which is locally asymptotically stable under these conditions for all $\theta > 0$, will attract all solutions. Finally, when the cleared infection steady state is locally asymptotically stable and the chronic steady state exists, *i.e.*, when

$$1 + \frac{p_A}{c} < 1 + \frac{\xi}{c} \bar{A}_5 < R_0 < 1 + \frac{\xi}{c} \Gamma, \quad (22)$$

we observe bistability of the cleared infection and chronic steady states S_4 and S_5 .

It is interesting to think of

$$R_0^a = R_0 - \frac{\xi}{c} \Gamma$$

as a new effective basic reproductive number giving the condition for chronic infection in the presence of antibodies. Indeed, when $R_0^a > 1$ the infection is sustained (as a chronic locally asymptotically stable steady state or a limit cycle). When $R_0^a < 1$, however, bistability between clearance and chronic steady states occurs when (22) is satisfied.

In the next section we will investigate these types of behaviors numerically.

Numerical results

Parameter values. After injury the liver can rapidly regenerate. We assume that during infection the maximum proliferation rate for uninfected hepatocytes is $r = 1 \text{ d}^{-1}$ [44], corresponding to approximately a division every 16 hours. The total number of hepatocytes in the liver, T_m , has been estimated at about 2×10^{11} [45], and assuming HBV can distribute throughout the 15 liters of extracellular fluid in the average 70 kg person, we normalize the liver cell population as done in previous models [9,46] so that we consider the cells responsible for producing virus in one ml. Hence, we take $T_m = 13.6 \times 10^6$ cells per ml. We use the estimates from earlier studies for the viral clearance rate, $c = 0.67 \text{ d}^{-1}$ [25,31]. We consider the entire liver to be susceptible to infection, $T_0 = T_m$, no initial infection $I_0 = 0$ and an HBV inoculum of $V_0 = 0.33$ virions per ml [9]. Each virion contains one HBV DNA molecule and typically HBV DNA per ml is measured as a surrogate for virions per ml.

The serum immunoglobulin IgG concentration in healthy adult individuals ranges between 7–17 mg/ml [47,48]. We assume that at most 10% of IgG levels are HBsAg-specific and thus set the antibody carrying capacity to 1 mg/ml for the HBsAg-specific antibody. The relative molecular mass of an IgG molecule is 150 kDa = 150,000 g/mol. Therefore there are a maximum of

$$\begin{aligned} A &= \frac{1\text{g}/1}{150000\text{g}/\text{mol}} = 6.7 \times 10^{-6} \text{mole}/1 \\ &= (6.7 \times 10^{-6}) \times (6.023 \times 10^{23}) \text{molecules}/1 \\ &= 4 \times 10^{18} \text{molecules}/1 = 4 \times 10^{15} \text{molecules}/\text{ml}. \end{aligned} \quad (23)$$

Hence, we set the HbsAg-specific antibody carrying capacity at $A_m = 4 \times 10^{15}$ molecules per ml. Initially, we assume there are no free or complexed HbsAg-specific antibodies present, *i.e.* $A_0 = 0$ and $X_0 = 0$. The IgG subclasses that form immune complexes with HBsAg have half-lives in blood of 21 days [49,50,51], corresponding to an antibody removal rate $d_A = \ln(2)/9.7 = 0.033/\text{day}$. We do not know the antigen-dependent and -independent antibody growth rates p_A and r_A which we estimate through data fitting. We take the virus-antibody dissociation rate to be 10^{-4} per second, or approximately $k_m = 10 \text{ d}^{-1}$ [52]. The IgG affinity $K = k_p/k_m$ in a humoral response frequently starts at 10^5 M^{-1} [53] and can become as high as 10^8 M^{-1} [54]. For HBV, each virion can have ten to hundreds of potential antibody binding sites and affinity maturation may occur. Taking both effects into account can increase the functional affinity K to 10^8 M^{-1} . Therefore, the binding rate $k_p = K \times k_m = 10^9 \text{ M}^{-1}/\text{day} = 10^{-12}$ ml per molecule per day. Below we also consider a model where multiple antibodies can bind each virus particle. The antibody-virus complex clearance rate is taken as four times higher than the clearance of the virus, *i.e.*, $c_{AV} = 4c = 2.7 \text{ d}^{-1}$, as has been found for HIV-antibody complexes [55].

There is 100-fold to 100,000-fold excess of noninfectious subviral particles, corresponding to θ , relative to infectious particles [19]. We assume that a healthy individual produces an excess of $\theta = 10^3$ subviral particles. We estimate the remaining parameters $\{\beta, \delta, \pi, p_A, r_A\}$ by fitting V as given by the antibody model (7) to data from HBV acute infections [56,9] and Table S1. The infection dates for each patient were either known or estimated previously [9,57]. We use the ‘fminsearch’ and ‘ode15s’ routines in MATLAB R2012a (The MathWorks Inc., Natick, MA). The

parameter values are presented in Tables 1 and 2. We then vary θ , r_A , p_A and A_0 and investigate the results.

Virus dynamics. In the absence of antibody responses $R_0 = \frac{\pi\beta T_m}{c\delta} > 1$, corresponding to established, chronic HBV infection in model (1). We investigate how these dynamics change in the presence of antibody and an excess of $\theta = 10^3$ subviral particles.

We fitted V as given by the antibody model (7) to data from seven individuals, who were identified in the acute stage of infection during a single-source HBV outbreak (for details see [56]). The results are presented in Fig. 1 and the best parameter estimates for each patient are presented in Table 2. The model matches the high viral peak observed during each patients’ acute infection phase, and the biphasic viral decay from the peak. Moreover, the best estimates predict that virus clearance (defined as less than one virion in the body) occurs following infection in the first six patients and does not occur in patient 7 (who is known to have developed chronic infections). Although the model fits the virus data, it predicts that free antibody levels are much higher than those observed in unvaccinated patients. We will show in section 4.4 how addition of a cell-mediated immune response allows for viral clearance with lower antibody concentrations.

We did not find any correlation between R_0 and the time to clearance, however the fast clearance time noticed in patient 1 corresponds to a steep second phase viral decay due to a high loss rate of infected cells, δ . Conversely, patients 3 and 7, who have the smallest δ , experience the longest time until viral clearance and no clearance, respectively.

The parameter estimates for the first six patients satisfy the condition $1 < R_0 < 1 + \frac{\xi}{c} \Gamma$ corresponding to asymptotic stability of the cleared infection steady state. Moreover, if $R_0 > 1 + \frac{\xi}{c} \Gamma$ the cleared infection steady state becomes unstable and either a stable chronic steady state or a limit cycle emerge (Fig. 2).

We next assume that all parameters values are fixed at the median best fit values given in Table 2, which satisfy the clearance conditions (19), and we investigate how the virus dynamics change when we vary four bifurcation parameters: the constant of proportionality θ , the antigen-independent and -dependent antibody growth rates r_A and p_A , and the initial antibody concentration A_0 . As θ increases it reaches a threshold value θ_c such that for $\theta < \theta_c$ virus is cleared and the antibody reaches its carrying capacity Γ (Fig. 3). For $\theta > \theta_c$ a chronic steady state value emerges which co-exists and is bistable with the cleared infection steady state (Fig. 4). In the bistable parameter space viral clearance is reached asymptotically when the antigen-independent antibody growth rate r_A is increased (see Fig. 5 left panel) or when initial antibody levels are increased (see Fig. 5 right panel). Similar results are obtained when the antigen-dependent growth rate p_A is increased (Fig. S1 in Text S1).

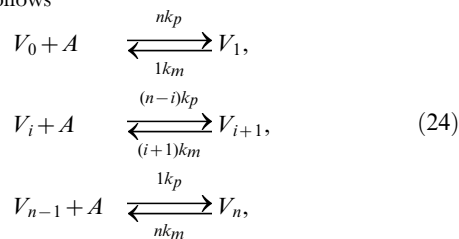
The antibody model (7) assumed that when one antibody binds a virus with a certain avidity the virus will be neutralized. Since HBV has multiple surface proteins, each of them can potentially facilitate infection. This situation has been described in HIV viral infection where even as little as one functional gp160 (surface protein) may be sufficient to promote virus entry [58,59]. We investigate the changes in the dynamics of model (7) if we incorporate binding to multiple surface proteins into model (7) as follows. Let V_0 be the concentration of virus with no antibody bound and V_i be the concentration of virus with i surface antigens bound by antibody, with $i = 0, 1, \dots, n$, where we assume n is the maximum number of antibodies that can simultaneously bind a virion. When V_i encounters an antibody, A , there are $n - i$ ways to occupy one of its surface proteins and obtain a virion with $i + 1$

Table 1. Variables, parameters and values used in simulations.

Variables		
T	Target cells	$T_0 = 13.6 \times 10^6$ per ml
I	Infected cells	$I_0 = 0$
A	Free antibody	molecules per ml (varies)
V	Free virus	$V_0 = 0.33$ per ml
S	Subviral particles	-
X	Virus-antibody complexes	$X_0 = 0$
X_S	Subviral particle-antibody complexes	-
Parameters		
r	hepatocyte maximum proliferation rate	1 d^{-1}
β	infectivity rate constant	ml d^{-1} (varies)
T_m	hepatocyte carrying capacity	13.6×10^6 cells per ml
δ	infected cell killing rate	d^{-1} (varies)
ρ	cure rate	0
p_A	antibody production	molecules d^{-1} (varies)
r_A	antigen-independent antibody growth rate	d^{-1} (varies)
d_A	antibody degradation rate	0.033 d^{-1}
A_m	antibody carrying capacity	4×10^{15} molecules per ml
k_p	antibody binding rate	$10^{-12} \text{ ml d}^{-1}$
k_m	antibody dissociation rate	10 d^{-1}
π	virus production rate	d^{-1} (varies)
c	virus clearance rate	0.67 d^{-1}
c_{AV}	complexes degradation rate	2.7 d^{-1}
θ	subvirus:virus ratio	varies
η	antibody units conversion factor	2.7×10^{-16} mg/molecule

doi:10.1371/journal.pcbi.1003730.t001

occupied sites, V_{i+1} . The reaction kinetics can be represented schematically as follows



where $i = 1, 2, \dots, n-2$. As before, k_p is the rate constant for binding between the antibody and a viral surface antigen and k_m is the disassociation rate. We consider that the virus-antibody complexes are cleared at a rate proportional to the number of bound antibodies, *i.e.*,

$$c_{AV}(i) = c(i+1), \tag{25}$$

or the effects of antibody binding on clearance saturate, *i.e.*,

$$c_{AV}(i) = c + c_1 \frac{i^h}{i_{50}^h + i^h}, \tag{26}$$

where h is a hill coefficient, c_1 is the maximum increase in clearance that can be obtained by antibody binding, and i_{50} is the number of bound antibodies needed to generate a half-maximal effect. Moreover, we assume that the virus-antibody complexes infectivity rates decrease with the number of bound antibodies [58,60,61]. Lastly, the SVPs

with i surface antigens bound by antibody are proportional with the virus with i bound antibodies, *i.e.* $S_i = \theta V_i$. System (7) becomes

$$\begin{aligned}
 \frac{dT}{dt} &= rT \left(1 - \frac{T+I}{T_m}\right) - T \sum_{i=0}^{n-1} \frac{\beta}{i+1} V_i, \\
 \frac{dI}{dt} &= T \sum_{i=0}^{n-1} \frac{\beta}{i+1} V_i - \delta I, \\
 \frac{dA}{dt} &= p_A(1+\theta) \sum_{i=0}^{n-1} V_i + r_A A \left(1 - \frac{A}{A_m}\right) - \\
 &\quad d_A A + (1+\theta) \sum_{i=1}^n \{ik_m V_i - (n-i+1)k_p V_{i-1} A\}, \\
 \frac{dV_0}{dt} &= \pi I - cV + k_m V_1 - nk_p V_0 A - cV_0, \\
 \frac{dV_i}{dt} &= (i+1)k_m V_{i+1} - (n-i)k_p V_i A - ik_m V_i + \\
 &\quad (n-i+1)k_p V_{i-1} A - c_{AV}(i) V_i, \\
 \frac{dV_n}{dt} &= k_p V_{n-1} A - nk_m V_n - c_{AV}(n) V_n,
 \end{aligned} \tag{27}$$

Table 2. Parameter best estimates.

Patient	$\beta \times 10^{-10}$	π	δ	r_A	$p_A \times 10^{-5}$	RSS
1	0.953	297	0.1538	0.4242	0.1	4.8
2	11.1	43.5	0.061	0.4656	0.7	3.5
3	18.2	12.4	0.018	0.2672	9	3.5
4	8.8	26.4	0.064	0.288	520	3
5	6.1	42.5	0.049	0.3578	10	2
6	5.87	28.5	0.043	0.29	1.16	8.1
7	2	113	0.0000998	0.4623	0.41	6.1
median	6.1	42.5	0.049	0.358	1.16	-
average	7.57	80.5	0.056	0.365	77.3	-
stdev	5.87	101	0.049	0.085	195	-

The parameter units are as described in Table 1.
doi:10.1371/journal.pcbi.1003730.t002

where $i = 1, 2, \dots, n$ and the $1 + \theta$ terms are included to account for the antibody binding to SVPs. The total HBV virus is $V_T = V_0 + \sum_{i=1}^n V_i$, the total immune complexes is $X = \sum_{i=1}^n V_i$ and the total antibody is $A_T = A + (1 + \theta) \sum_{i=1}^n i V_i$. We will refer to system (27) as the multivalent binding model.

It has been reported that quasispherical SVP contain 48 HBsAg dimers [23] and we assumed that virions have the same HBsAg numbers. We compared the dynamics of virus and antibody-virus complexes as given by the multivalent binding model (27) for $n = 1$, $n = 50$ and $c_{AV}(i)$ given by (25) or (26) with $c_1 = 3c$, $h = 1$ and $i_{50} = n/2$. To preserve the avidity of the antibody we normalize the binding and unbinding parameters so that nk_p/k_m is constant. For $n = 50$ we assume $k_p = 2 \times 10^{-14}$ and $k_m = 10$. Numerical results show that the exponential growth to the peak and the rates of first and second phase decay of both virus and total virus-antibody complexes are similar regardless of n (Fig. 6). However, the overall levels of free virus and total antigen-antibody complexes during the second phase decay decrease for high n due to faster clearance of immune complexes for both forms of $c_{AV}(i)$ (Fig. 6).

Antibody dynamics. We investigated the dynamics of free antibodies, virus-antibody and subviral particle-antibody complexes for the antibody model (7) and the median parameter values given in Tables 1 and 2 and various values of θ , r_A , p_A and A_0 . We present antibody concentrations in mg per ml by multiplying the antibody values obtained in simulations by a factor $\eta = 2.7 \times 10^{-16}$ which transforms molecules/ml to mg/ml, and takes into account the molecular weight of IgG.

To understand the role of subviral particles, we first examine system (7)'s dynamics when the ratio of subviral particles to virus is $\theta = 10^3$ and the clearance condition (19) holds. As shown in Fig. 7, left panel, the HBsAg-specific antibody concentration is small, 1.14×10^{-6} mg/ml at day 82, when the virus is at its maximum. Antibody concentration continued to increase and reached its carrying capacity of 1 mg/ml two months after the virus peak, which is higher than reported in unvaccinated patients (Fig. 7 left panel).

When $\theta = 10^5 > \theta_c$ bistable dynamics emerge. When there are no pre-existing antibodies, $A_0 = 0$, the antibody is inefficient in controlling the virus. Even though free antibodies reach a maximum value of 1.17×10^{-7} mg/ml three weeks before the viral peak, this

equilibrium value is seven-order magnitude smaller than the antibody carrying capacity. This reduction in free antibody is due to the presence of subviral particles, which bind antibody and are rapidly cleared. Because of low antibody concentration and the rapid clearance of subviral particles the peak concentrations of virus-antibody and subviral particle-antibody complexes are also small, *i.e.*, 7.5×10^{-13} and 7.5×10^{-8} mg/ml, respectively (Fig. 7 middle panel), below the antibody's limit of detection of 0.1 ng/ml [62]. Moreover, virus clearance does not occur because the high level of subviral particles serve as a decoy binding the initially low number of antibodies. This leaves a window of opportunity for viral persistence.

When $\theta = 10^5 > \theta_c$ and $A_0 = 2 \times 10^4$ molecules/ml (5.4×10^{-12} mg/ml) we recover the same dynamics for virus, antibody and virus-antibody complexes as seen in the $\theta = 10^3$ case together with subviral particle-antibody complexes levels five orders of magnitude higher than those of virus-antibody complexes (Fig. 7 right panel).

The antibody model (7) assumed that B-cell priming by the virus is followed by an antigen-independent antibody expansion with a maximum per capita growth rate r_A . This was one of the parameters that we fitted to the data and obtained estimates ranging between 0.26 d^{-1} and 0.46 d^{-1} . To determine how the dynamics of the antibody model (7) change if we vary r_A , we kept all the other parameters fixed at the median values in Tables 1 and 2 and assumed $\theta = 10^3$ and $A_0 = 0$. As seen in Fig. 8, the virus is cleared when the antibody growth rate r_A is high. However, as r_A decreases the time to viral clearance increases until, eventually, the virus cannot be controlled and chronic infection occurs (Fig. 8, dotted lines). The chronicity can be reversed when the initial antibody level is increased (Fig. 9, right panel), as occurs after vaccination. Similar dynamics are seen when the antigen-dependent antibody growth rate p_A is varied.

We assumed that the antibody parameters p_A and r_A are unknown. By calculating the relative sensitivity equations with respect to p_A and r_A [63], we find that the effects of p_A and r_A on the virus, antibody and virus-antibody complexes are proportional at each time point (Fig. S3 in Text S1). Therefore fixing one and fitting the other will preserve virus-antibody dynamics. The combined effects of r_A and p_A on the virus steady state are presented in Fig. S1 in Text S1. Moreover, the model long-term's outcomes do not

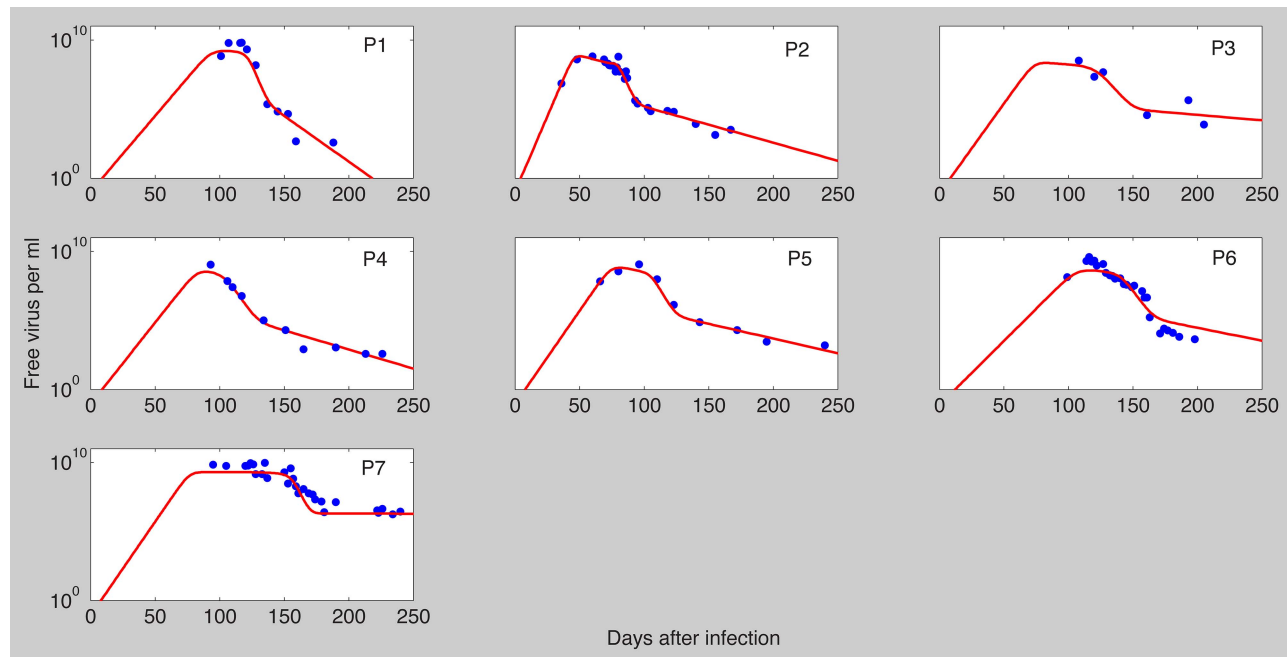


Figure 1. The best fit of V as given by model (7) (solid lines) to patient data (•). Best parameter estimates are presented in Table 2. The other parameters are as in Table 1.
doi:10.1371/journal.pcbi.1003730.g001

change when the antibody affinity $K = k_p/k_m$ is constant, but the relative k_p and k_m values vary within reasonable ranges (not shown).

Because r_A is a surrogate for the B cell growth rate and is also an important parameter in determining whether viral clearance or chronicity occurs, we investigated the changes in our results when we expand the antibody model (7) to include

the dynamics of activated (B) and memory (M) B cells. We assume that activated B cells expand at rate p_B proportional to viral and subviral concentrations, die at rate d_B , and become memory cells at rate α . Memory cells are maintained through antigen-independent homeostatic proliferation with a maximum difference between proliferation and loss rate r_M , and

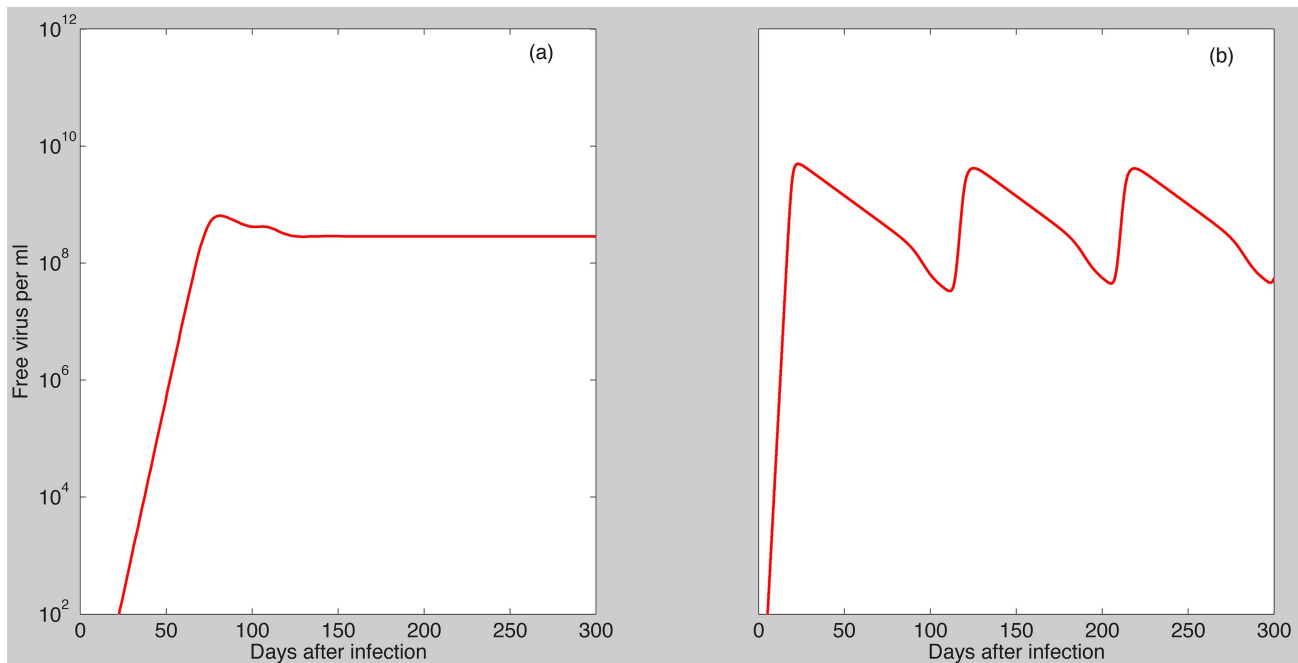


Figure 2. Dynamics of V as given by model (7) when the cleared infection condition (19) fails. Parameter values are as in Table 1 and $A_m = 4 \times 10^{12}$ molecules per ml, $\theta = 10^3$, $\beta = 6.1 \times 10^{-10}$ ml per virus per day, $\delta = 0.0494 \text{ d}^{-1}$, $r_A = 0.358 \text{ d}^{-1}$, $p_A = 1.16 \times 10^{-5}$ molecules d^{-1} , $\pi = 42.5$ per infected cell per day (panel a); $\pi = 300$ per infected cell per day (panel b).
doi:10.1371/journal.pcbi.1003730.g002

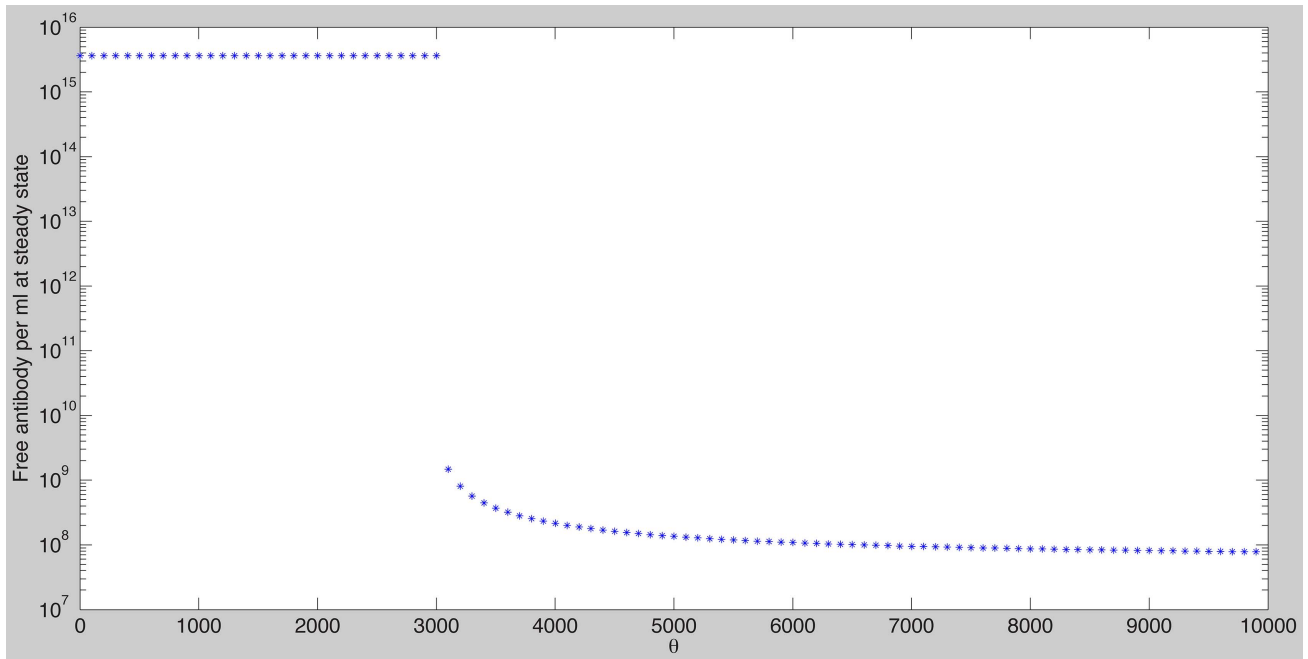


Figure 3. Free antibody at steady state as given by model (7) as a function of θ . The other parameters are as Tables 1 and 2 (median values). Note that for $\theta < 3000$, the antibody reaches its carrying capacity Γ . For $\theta > 3000$ the infection is not cleared and the maximum antibody value is less than the carrying capacity Γ .
doi:10.1371/journal.pcbi.1003730.g003

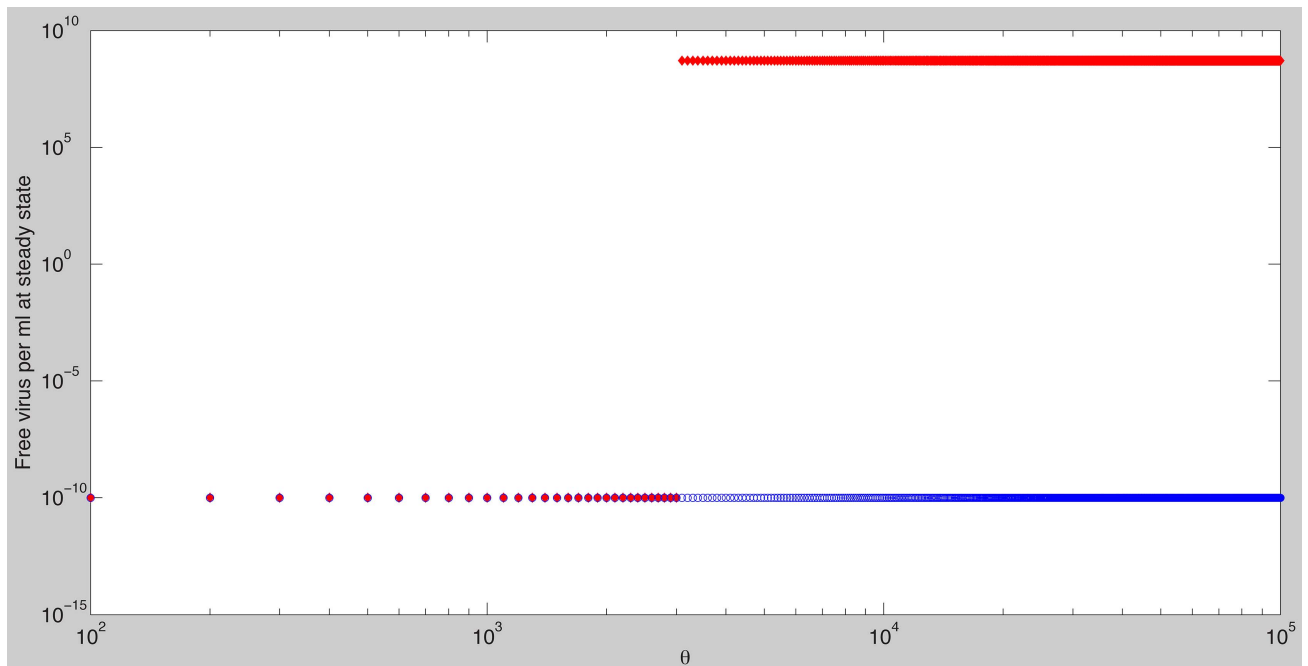


Figure 4. Stable steady state solutions for V as given by model (7) as a function of θ . The other parameters are as in Tables 1 and 2 (median values). Notice bistability between the chronic and the cleared infection steady states occurs when $\theta > \theta_c = 3.1 \times 10^3$. The cleared infection steady state is reached for all θ when $A_0 = 10^8$ molecules per ml.
doi:10.1371/journal.pcbi.1003730.g004

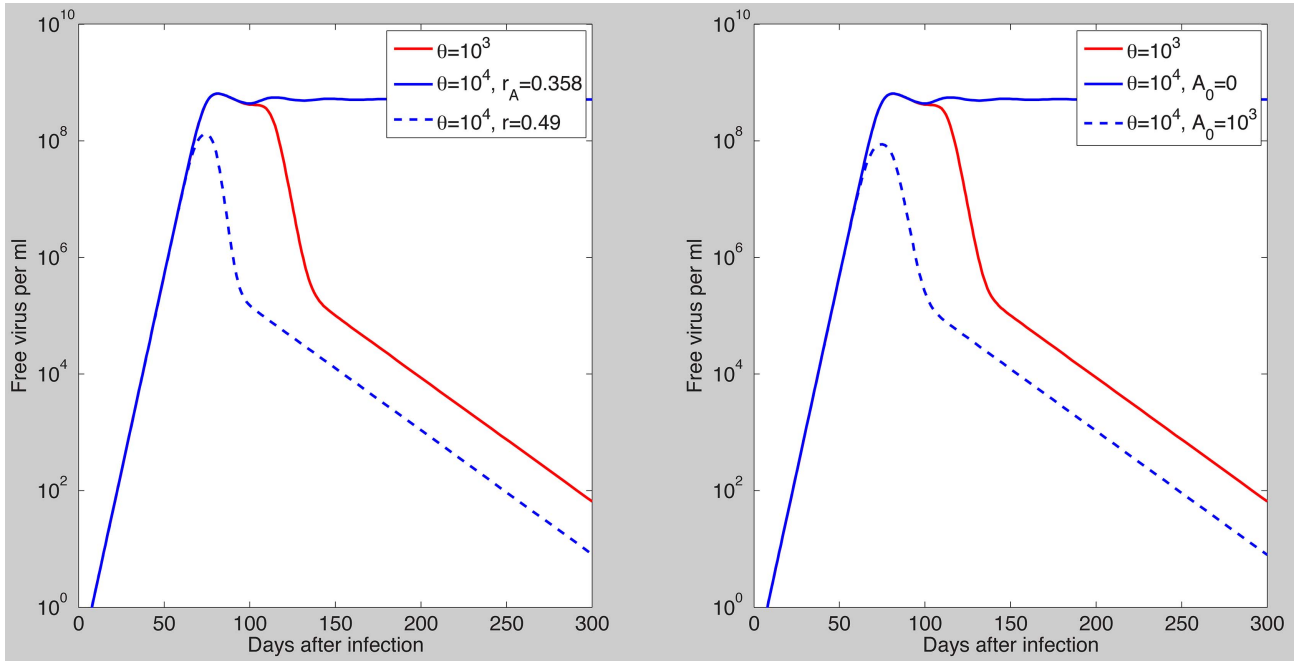


Figure 5. Free virus dynamics as given by model (7) and parameters in Tables 1 and 2 (median values): The asymptotically stable cleared infection steady state is approached for $\theta=10^3$ (red line, both panels); bistable dynamics is observed for $\theta=10^4$ with (left panel): Viral clearance for $r_A=0.49 d^{-1}$ and $A_0=0$ (dashed blue line) and viral persistence for $r_A=0.358 d^{-1}$ and $A_0=0$ (solid blue line); (right panel): Viral clearance is observed for $r_A=0.358 d^{-1}$ and $A_0=10^3$ molecules per ml (dashed blue line) and viral persistence for $r_A=0.358 d^{-1}$ and $A_0=0$ molecules per ml (solid blue line). doi:10.1371/journal.pcbi.1003730.g005

carrying capacity M_m . Antibody is produced at rates s_B and s_M by naive and memory B cells, respectively and is eliminated at rate d_A . The virus-antibody complex formation is identical to that of model (7). The expanded model (called the B cell activation model),

$$\begin{aligned}
 \frac{dT}{dt} &= rT(1 - \frac{T+I}{T_m}) - \beta VT, \\
 \frac{dI}{dt} &= \beta VT - \delta I, \\
 \frac{dB}{dt} &= p_B(1 + \theta)V - d_B B - \alpha B, \\
 \frac{dM}{dt} &= \alpha B + r_M M(1 - \frac{M}{M_m}), \\
 \frac{dA}{dt} &= s_B B + s_M M + (1 + \theta)k_m X - (1 + \theta)k_p AV - d_A A, \\
 \frac{dX}{dt} &= -k_m X + k_p AV - c_{AV} X, \\
 \frac{dV}{dt} &= \pi I - cV + k_m X - k_p AV,
 \end{aligned}
 \tag{28}$$

has essentially the same dynamics as the antibody model (7). Indeed, viral clearance occurs when

$$R_0 < 1 + \frac{\xi r_M M_m}{c d_A}.
 \tag{29}$$

Moreover, bistability between the cleared and the chronic infection steady states emerges when θ is high and virus clearance occurs when initial antibody levels A_0 or antibody production rates s_B and s_M are increased (not shown).

Model of combined antibody and cellular immune responses. In our study of the antibody model (7) and its variants, we found that we can describe the data, including the transient nature of primary HBV infection, by the effect of antibodies. However, in every case, a large concentration of antibodies was needed relatively early, reflected for example in a high initial level (A_0), a fast growth rate (r_A) of antibodies, a high affinity ($K_A = k_p/k_m$), or a high antibody carrying capacity (A_m). But in clinical practice, antibodies are not detectable until the virus is well on its way to being cleared. Thus, it is possible that another mechanism of control needs to be included. We now investigate this by expanding model (7) to include the effects of effector CD8 T-cells (E), along the lines of our previous work [9].

We assume that in the absence of infection there is a basal level of HBV-specific immune effector cells given by s_E/d_E , where s_E are CD8 T cells specific for HBV-infected cells and $1/d_E$ is their average lifespan. Upon encounter with antigen CD8 T cells are activated, clonally expand, and differentiate into true effector cells at rate α_E . We assume that there is a time delay, τ , between antigen encounter and effector cell expansion as in [9]. Infected cells can be killed by the immune response at a rate of μE per cell. The new CD8-antibody model is

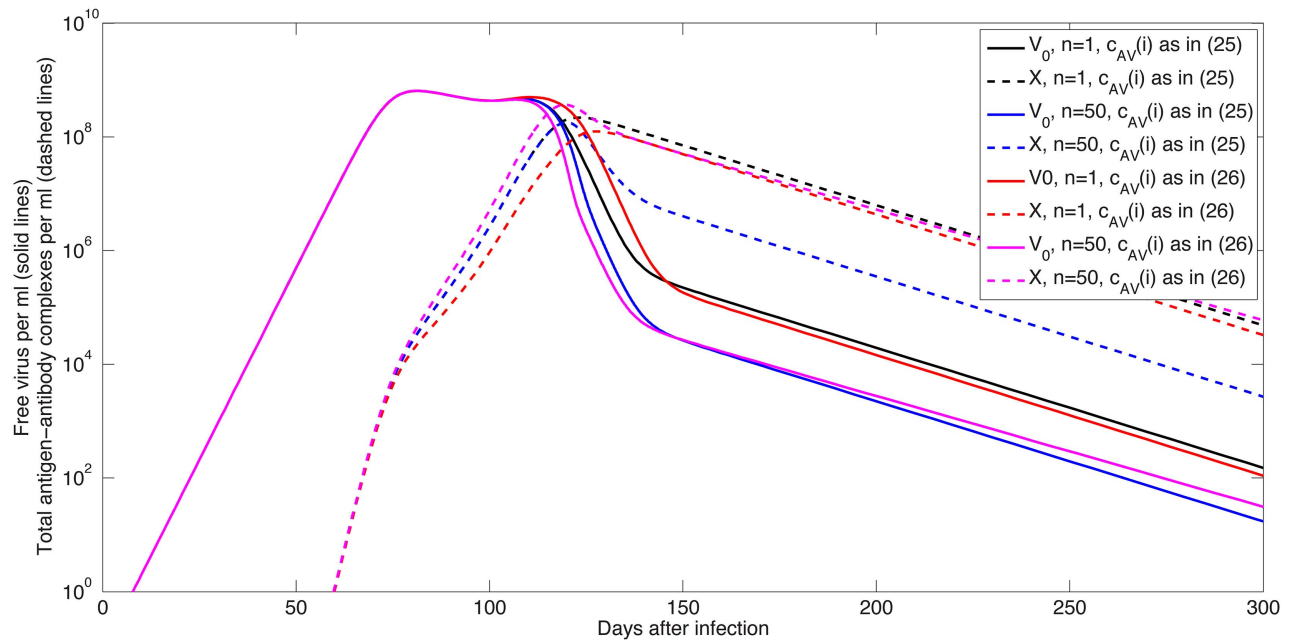


Figure 6. Free virus V_0 (solid lines) and total complexes $\sum_{i=1}^n V_i$ (dashed lines) as given by model (27) for $n=1, n=50, c_{AV}(i)$ given by (25) (black and magenta lines) and $c_{AV}(i)$ given by (26) with $c_1 = 3c, h=1$ and $i_{50}=n/2$ (red and blue lines). The binding and unbinding rates are normalized so that nk_p/k_m is constant. The other parameters are as in Tables 1 and 2 (median values). doi:10.1371/journal.pcbi.1003730.g006

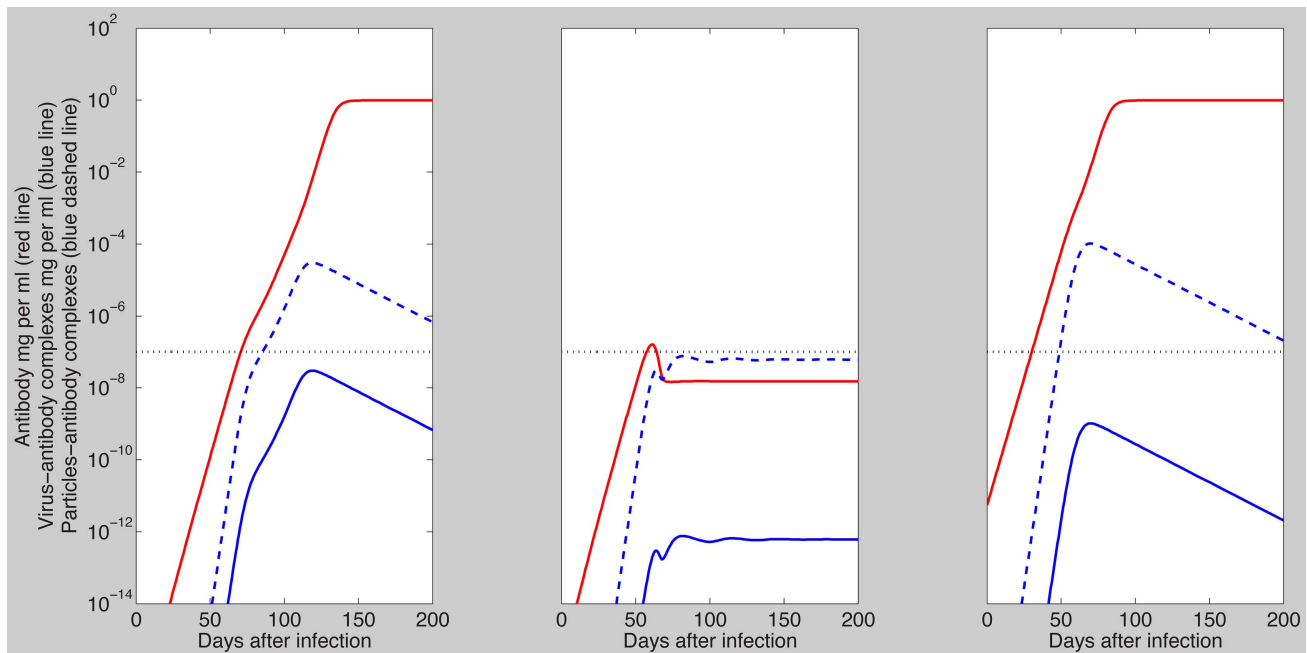


Figure 7. Free antibody (red lines), virus-antibody complexes (solid blue lines) and subviral particles-antibody complexes (dashed blue lines) in mg/ml as given by model (7) and parameters in Tables 1 and 2 (median values) for $\theta = 10^3, A_0 = 0, r_A = 0.358 \text{ d}^{-1}$ (left panel); $\theta = 10^5, A_0 = 0 \text{ mg/ml}, r_A = 0.358 \text{ d}^{-1}$ (middle panel); $\theta = 10^5, A_0 = 2 \times 10^4 \eta \text{ mg/ml}, r_A = 0.358 \text{ d}^{-1}$ (right panel). The dotted black line represents the antibody limit of detection of 0.1 ng/ml and $\eta = 2.7 \times 10^{-16}$ is the factor transforming the units from molecules/ml to mg/ml. doi:10.1371/journal.pcbi.1003730.g007

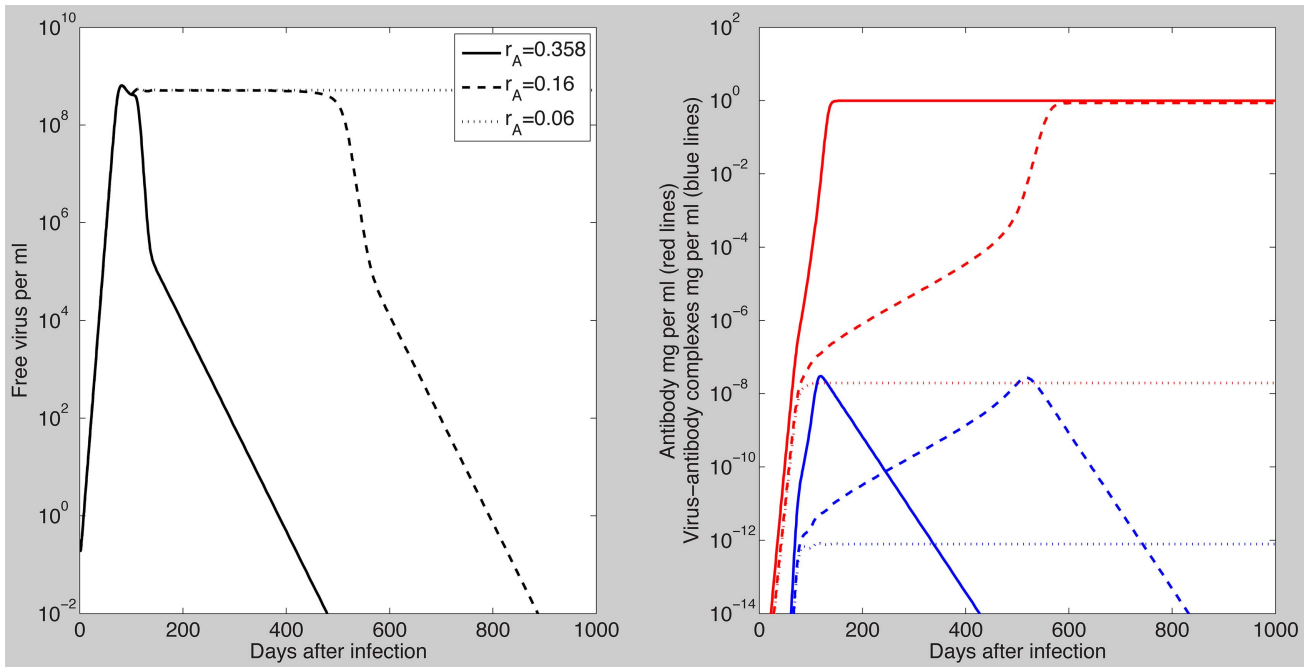


Figure 8. Free virus per ml (left panel); free antibody (red lines) and virus-antibody complexes (blue lines) in mg/ml (right panel) for $r_A = 0.358 \text{ d}^{-1}$ (solid lines); $r_A = 0.16 \text{ d}^{-1}$ (dashed lines) and $r_A = 0.06 \text{ d}^{-1}$ (dotted lines). The other parameters are as Tables 1 and 2 (median values).
doi:10.1371/journal.pcbi.1003730.g008

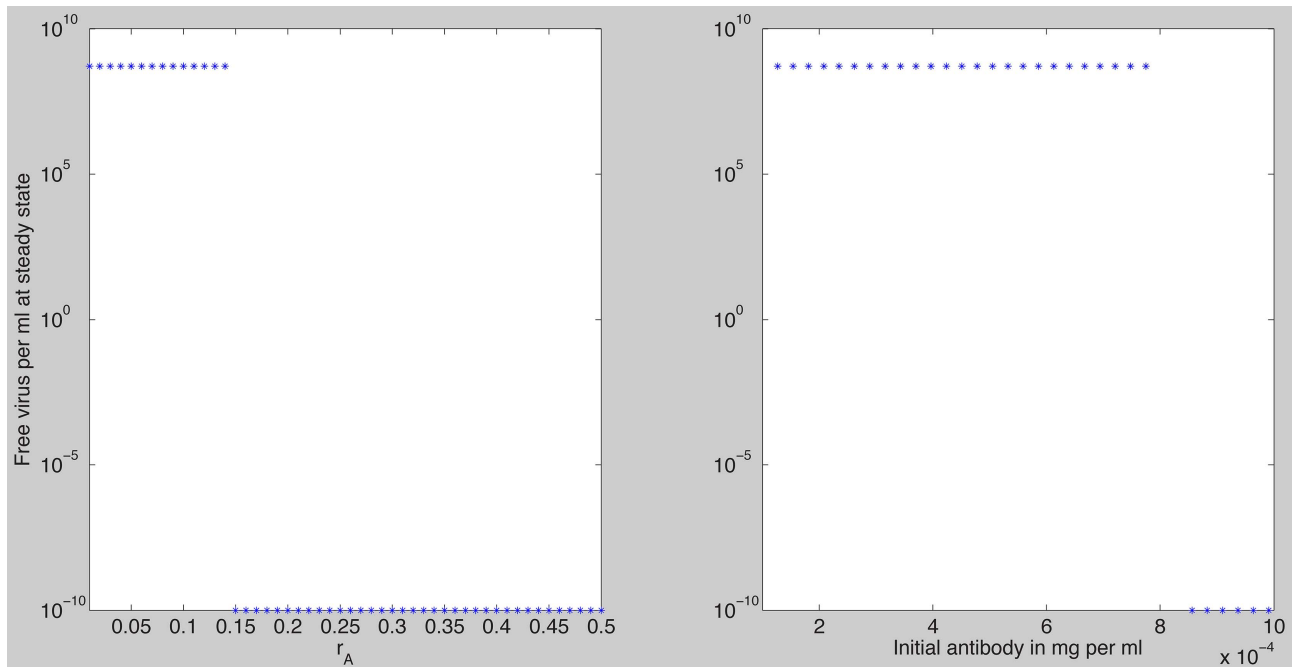


Figure 9. Stable steady state solutions for free virus, V , as given by model (7), for $\theta = 10^3$ as a function of r_A when $A_0 = 0$ (left panel), and A_0 when $r_A = 0.04167 \text{ d}^{-1}$ (right panel). The other parameters are as in Tables 1 and 2 (median values).
doi:10.1371/journal.pcbi.1003730.g009

Table 3. Estimated parameters found by fitting model (30) to data.

Patient	$\beta \times 10^{-10}$	π	δ	r_A	$p_A \times 10^{-3}$	$\mu \times 10^{-3}$	RSS
1	2.54	266.8	0.11	0.31	8.8	2.1	4.99
2	9.24	117.1	0.035	0.29	5.9	2.5	3
3	6.23	159.4	0.071	0.24	13.8	0.6	3.27
4	4.9	365.5	0.146	0.45	0.1	1	2.43
5	4.95	186.7	0.082	0.41	0.9	0.6	3.33
6	2.21	327.3	0.073	0.22	1.5	0.5	7.14
7	2.6	305	0.018	0.35	0.1	0.1	6.9
median	4.85	266	0.073	0.31	1.5	0.6	-
average	4.65	246	0.076	0.32	4.4	1	-
stdev	2.53	93	0.042	0.08	5.3	0.9	-

doi:10.1371/journal.pcbi.1003730.t003

$$\begin{aligned}
 \frac{dT}{dt} &= rT\left(1 - \frac{T+I}{T_m}\right) - \beta VT, \\
 \frac{dI}{dt} &= \beta VT - \delta I - \mu IE, \\
 \frac{dA}{dt} &= p_A(1+\theta)V + r_AA\left(1 - \frac{A}{A_m}\right) + \\
 &\quad (1+\theta)k_mX - (1+\theta)k_pAV - d_AA, \\
 \frac{dX}{dt} &= -k_mX + k_pAV - c_{AV}X, \\
 \frac{dV}{dt} &= \pi I - cV + k_mX - k_pAV, \\
 \frac{dE}{dt} &= s_E - d_EE + \alpha_E I(t-\tau)E(t-\tau),
 \end{aligned}
 \tag{30}$$

with $E(0) = s_E/d_E$, $s_E = 30$ cells per day, $d_E = 0.5$ per day and $\alpha_E = 2.2 \times 10^{-7}$ per infected cells per day as in [9]. Moreover, we assume that the free and bound virus is cleared at rates $c = 1.67$ and $c_{AV} = 4c$ per day. The antibody binding rate is $k_p = 10^{-10}$ per molecules per day, two-fold higher than in the antibody model (7) and the antibody carrying capacity $A_m = 4 \times 10^{11}$ is four-fold lower than in the antibody model (7). This allows for a higher antibody affinity that can control the infection even at low equilibrium antibody levels. As before, a healthy individual produces an excess of $\theta = 10^3$ subviral particles. We assume that the delay in the expansion of effector cells is kept at values given in [9], *i.e.*, $\tau_{\text{patient}_i} = \{15.2, 19.6, 29, 34.4, 16.8, 29.7, 33.4\}$, $i = 1, \dots, 7$, and estimate the remaining parameters $\{\beta, \delta, \pi, p_A, r_A, \mu\}$ by fitting V to data from HBV acute infections [56,9]. The estimates are presented in Table 3 and the free virus and free antibody are presented in Fig. 10 (red and green lines, respectively). We note that due to the complexity of the CD8-antibody model, the estimates obtained (with Matlab’s ‘fminsearch’, as before) are consistent with the data, but we do not claim a unique solution, since for example we fixed many of the parameters as described.

In the CD8-antibody model, the cellular immune responses are responsible for the initial virus decay and antibodies that bind virus with high affinity, $K = k_p/k_m = 10^{-11}$ molecules per mL (10^{10} M^{-1}) control the second phase decay and prevent virus rebound (Fig. 10 red lines, first six patients). This result holds even though the overall antibody level is small, with free antibody growing above the limit of detection 90–172 days after infection and reaching an equilibrium of 10^{-4} mg per mL, four-fold lower than in model (7) (Fig. 10 green lines, first six patients).

When both the antibody production rate, p_A , and the CD8 T cell killing rate, μ , are small (97.7 and 75.5 times smaller than the average values among the patients), model (30) predicts virus rebound (Fig. 10 red line, patient 7) and low levels of free antibody (Fig. 10 green line, patient 7).

Therefore, virus clearance can be obtained for high equilibrium antibody levels alone, or for low equilibrium antibody levels combined with a potent cellular immune response.

Discussion

We developed a set of mathematical models of the antibody response to hepatitis B viral infection and tested whether viral clearance is possible in the presence of an excess number of

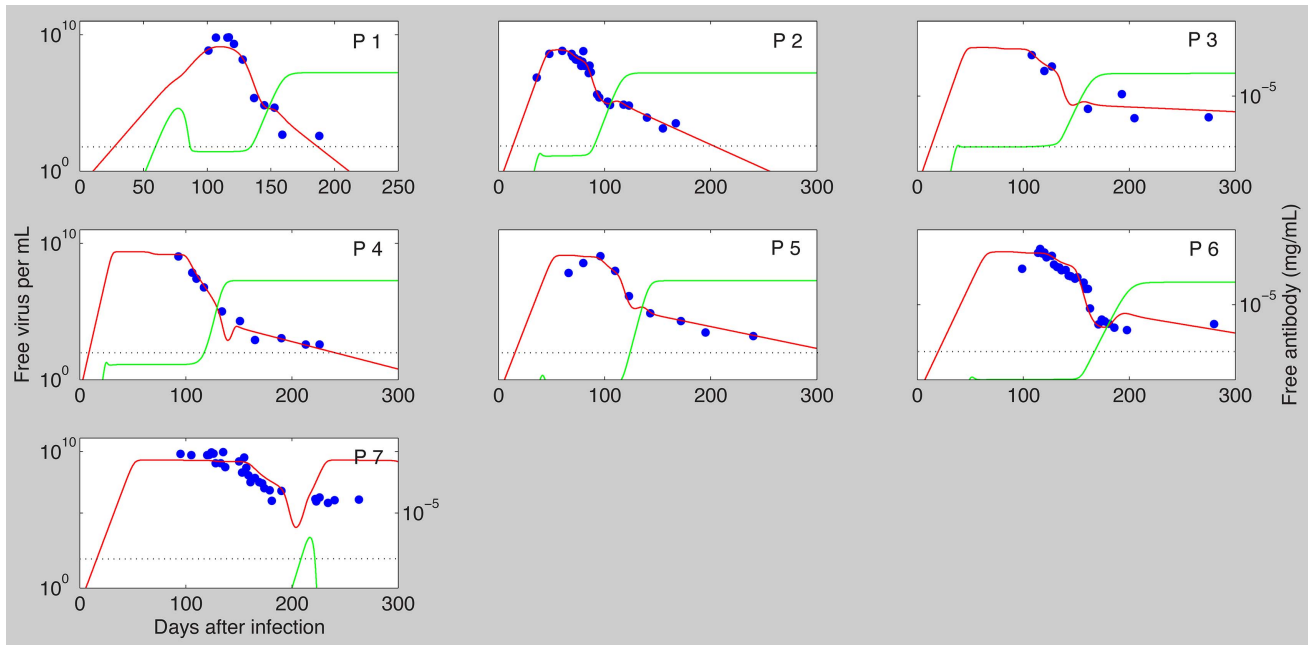


Figure 10. The viral load (red lines) and free antibody (green lines) predicted by model (30). The dotted line represents the antibody limit of detection of 0.1 ng per mL. Best parameter estimates are presented in Table 3. $k_p = 10^{-10}$ per molecule per day, $A_m = 4 \times 10^{11}$ molecules per mL, $c = 1.67$ per day, $c_{AV} = 4c$ per day and the other parameters are as in Table 1. Patient data is represented by blue symbols. doi:10.1371/journal.pcbi.1003730.g010

subviral particles. Subviral particles are non-infectious but have HBsAg on their surface and thus bind anti-HBV antibody. If they bind enough anti-HBV antibody they have the potential to counter the antibody response. We used the models and data from seven acutely infected patients to determine important parameters that describe virus and antibody dynamics.

Models of HIV have considered the antibody's effect on virus indirectly by modeling opsonization through enhanced viral clearance and neutralization through decreased virus infectivity [64,65]. Others considered in detail the interaction between virus and antibody that leads to complex formation [64]. Here, for the case of HBV, we modeled complex formation between antibody and both viral and subviral particles. This antibody model suggests that viral clearance is highly dependent on the characteristics of the antibody response: equilibrium antibody level, affinity, antigen-dependent and -independent antibody growth rates.

The antibody model (7) predicts that, for the same antibody dynamics, virus clearance can occur for low SVP:virus ratios but not for high SVP:virus ratios. However, viral clearance can be achieved regardless of the SVP:virus ratio if enough HBsAg-specific antibody is present at the time of infection or the antigen-dependent/-independent antibody growth rate is high enough. If we consider, as in clinical observations, that a healthy individual who produces an excess of $\theta = 10^3$ -particles very likely clears the infection, than virus clearance occurs in the absence of pre-existent antibody when the antibody population's doubling time is faster than 4.6 days (Fig. 9 left panel). Moreover, the virus can still be cleared for slow antibody expansion if vaccine induced antibodies are present at the time of infection [66]. It is thought that following hepatitis B vaccination and boosting, patients with anti-HBsAg levels of 10 mIU/ml (8.5×10^{-4} mg/ml) or higher are protected from infection [67,68,69]. In our study, if we assume an antibody population's doubling time of 16.6 days, the presence of HBsAg-

specific antibody levels higher than $A_0 = 8.5 \times 10^{-4}$ mg/ml leads to virus clearance (Fig. 9 right panel).

We assumed that the antibody's carrying capacity is fixed at the maximum antibody levels observed after vaccination and boosting. Moreover, we assumed that the initial inoculum is low and fixed among all patients. Under these conditions we obtained virus clearance in the absence of pre-existent antibody in six out of seven patients. The predicted antibody levels needed for clearance, however, are higher than observed clinically in unvaccinated individuals, where free antibodies are usually only detected after HBV is nearly cleared. If the predicted free antibody levels are decreased substantially (through decrease of activation parameters r_A and p_A or through decrease of the carrying capacity A_m) then pre-existent antibodies are required for protection (Figs. S1 and S2 in Text S1).

The antibody model (7) predicts that more than 45% of hepatocytes are infected at the peak of acute infection, lower than previously estimated [9]. These cells are replaced through homeostasis and the maximum liver loss at any one time ranges between 2 – 68%. The length of time the continuous liver death and replacement occurs is dependent on the antibody dynamics, such as the antigen-dependent and -independent growth rates r_A and p_A , and the initial values, A_0 . Rapid liver cell turnover can lead to accumulation of mutations in the host genome that could result in genetic alterations, chromosomal rearrangements, activation of oncogenes, inactivation of tumor suppressor genes, and ultimately to hepatocellular carcinoma as seen in many patients with chronic hepatitis [70].

Model (7) assumed that one antibody is sufficient to neutralize a virion. We relaxed this assumption by developing a multivalent model (27) that accounted for multiple binding events. We tested whether the observed dynamics change when multiple antibodies bind a virion and consequently lower virus infectivity and/or enhance virus clearance. We found that such antiviral activity has an effect on the size (but not the shape) of free and bound virus

during the second phase decay but not on viral peak (Fig. 6). Another antiviral response that we tested was the effect of increasing the ratio between the clearance of immune complexes and that of free virus. Originally we assumed that the immune complexes are cleared four times faster than the free virus, as in HIV [55]. In the virus clearance region, an increase in this ratio led to the decrease of free virus during the second phase decay (Fig. S4 in Text S1).

An unresolved issue is whether the assay used to measure patients HBV levels (the Amplicor HBV Monitor Test [57]) measures only free virus, as we assumed, or both HBV DNA in free virus and immune complexes. In this regard, the patient HBV DNA was recovered from serum samples by a chemical denaturant method [56], which has lower yield than techniques that use both chemical methods and proteolytic enzymes [71]. The latter should be more efficient at breaking apart virus-antibody complexes.

We compared the estimates for the other parameters with those from our previous hepatitis B study that used the same patient data [9]. We found that the median infectivity rate is higher, and the viral production rate is smaller in the antibody model (7). Our best estimates predict viral clearance in the first six patients and viral persistence in patient 7. This is consistent with clinical results which report that patient 7 was immunosuppressed and developed chronic disease. Data fitting shows that he has the lowest infected cell clearance rates. The antibody model (7) shows that in order for the virus to be cleared this patient would need to have one or a combination of the following: (1) low subviral particles production together with a high pre-existing antibody level; (2) antibody of high affinity; (3) high antigen-dependent and/or -independent antibody growth; (4) increased clearance of virus-antibody complexes; (5) increased loss of infected cells.

One important finding was that to obtain clearance of HBV, as observed in patients 1 to 6 and a majority of acutely infected adults, one needs high levels of antibody, higher than usually found in clinical observation. An alternative hypothesis for the effect of antibody is that they help clear the infection, once cellular immunity controls the initial burst of replication. The CD8-antibody model shows that cytotoxic effects lead to the initial viral control, and antibodies prevent re-infection. Previously, we had shown that a refractory/immune state of target cells could preserve the integrity of the liver while preventing re-infection [9]. Here we argue that antibodies could have a similar effect, with dynamics compatible with the observed levels and timing of antibodies in patients. Which of these effects is dominant, or if potentially both contribute to control of infection, needs further experimental studies.

One limitation of model (30) is that, for patients 2 to 7, killing of infected hepatocytes by CD8 T cells leads to more than 85% liver

loss. Therefore non-cytotoxic CD8 T cells effects leading to infected cells being cured and refractory to reinfection are needed to preserve liver integrity.

In summary, we have developed a set of models of hepatitis B infection that give insight into the opposing roles of antibody and subviral particles in the resolution of acute HBV infection. In particular, we showed that even when the virus produces a large number of subviral particles, as a decoy against antibody protection, viral clearance can still be achieved when pre-existing immunity induced through vaccination or cross immunity leads to the presence of high antibody levels early in infection. However, in individuals with low initial antibody levels, as in most unvaccinated individuals and in individuals without prior exposure to HBV, antibodies could have more of a mop up function, clearing the infection and preventing viral resurgence after a cellular immune response controls the initial infection.

Supporting Information

Code S1 Sample of code used to fit model (7) to the data. (DOCX)

Figure S1 Stable steady state solutions for free virus, V , as given by model (7), as a function of r_A and p_A for $\theta = 10^3$, $A_0 = 0$. The other parameters are as Tables 1 and 2 (median values). (EPS)

Figure S2 Stable steady state solutions for free virus, V , as given by model (7), as a function of θ and A_m for $\theta = 10^3$, $A_0 = 0$. The other parameters are as in Tables 1 and 2 (median values). (EPS)

Figure S3 The relative sensitive curves $q \frac{dZ}{dq}$ for $q = p_A$ (red lines) and $q = r_A$ (blue lines) and $Z = V$ (left panel), $Z = A$ (middle panel), $Z = X$ (right panel). The parameters are as in Tables 1 and 2 (median values). (EPS)

Figure S4 Free virus dynamics as given by model (7) for $c_{AV} = 4c$ (solid line), $c_{AV} = 10c$ (dashed line) and $c_{AV} = 150c$ (dotted line). $\theta = 10^3$, $A_0 = 0$, $r_A = 0.5$, and the other parameters are as Tables 1 and 2 (median values). (EPS)

Text S1 Supplementary information. (PDF)

Author Contributions

Conceived and designed the experiments: SMC RMR ASP. Performed the experiments: SMC. Analyzed the data: SMC. Contributed reagents/materials/analysis tools: SMC. Wrote the paper: SMC RMR ASP.

References

- Hollinger F, Liang T (2001) Fields Virology, Philadelphia: Lippincott Williams & Wilkins. 4th edition, pp. 2971–3036.
- Rehermann B, Nascimbeni M (2005) Immunology of hepatitis B virus and hepatitis C virus infection. *Nat Rev Immunol* 5:215–229.
- Waters J, Pignatelli M, Galpin S, Ishihara K, Thomas H (1986) Virus-neutralizing antibodies to hepatitis B virus: The nature of an immunogenic epitope to the S gene peptide. *J Gen Virol* 67:2467–2473.
- Ferrari C, Penna A, Bertolotti A, Valli A, Antoni A, et al. (1990) Cellular immune response to hepatitis B virus encoded antigens in acute and chronic hepatitis B virus infection. *J Immunol* 145:3442–3449.
- Guidotti L, Ishikawa T, Hobbs M, Matzke B, Schreiber R, et al. (1996) Intracellular inactivation of the hepatitis B virus by cytotoxic T lymphocytes. *Immunity* 4:25–36.
- McClary H, Koch R, Chisari F, Guidotti L (2000) Relative sensitivity of hepatitis B virus and other hepatotropic viruses to the antiviral effects of cytokines. *J Virol* 74:2255–2264.
- Wieland S, Eustaquio A, Whitten-Bauer C, Boyd B, Chisari F (2005) Interferon prevents formation of replication-competent hepatitis B virus RNA-containing nucleocapsids. *Proc Natl Acad Sci USA* 102:9913–9917.
- Wieland S, Guidotti L, Chisari F (2000) Intrahepatic induction of Alpha/Beta interferon eliminates viral RNA-containing capsids in hepatitis B virus transgenic mice. *J Virol* 74:4165–4173.
- Ciupe S, Ribeiro R, Nelson P, Dusheiko G, Perelson A (2007) The role of cells refractory to productive infection in acute hepatitis B viral dynamics. *Proc Natl Acad Sci USA* 104:5050–5055.
- Guo J, Zhou H, Liu C, Aldrich C, Saputelli J, et al. (2000) Apoptosis and regeneration of hepatocytes during recovery from transient hepatitis B virus infections. *J Virol* 74:1495–1505.
- Chisari F (2000) Viruses, immunity, and cancer: lessons from hepatitis B. *Am J Pathol* 156:1117–1132.
- Bertolotti A, Ferrari C (2003) Kinetics of the immune response during HBV and HCV infection. *Hepatology* 38:4–13.

13. Lai C, Locarmini S (2002) Hepatitis B virus. London, UK: International Medical Press.
14. Anh-Tuan N, Novk E, Holln S (1980) Hepatitis B surface antigen circulating immune complexes (HBsAg-CICs) in patients with bleeding disorders. *J Immunol Meth* 35:307–318.
15. Brown S, Steward M, Viola L, Howard C, Murraylyon I (1983) Chronic liver disease: the detection and characterization of circulating immune complexes. *Immunology* 49:673–683.
16. Glebe D, Lorenz H, Gerlich W, Butler S, Tochkov I, et al. (2009) Correlation of virus and host response markers with circulating immune complexes during acute and chronic woodchuck hepatitis virus infection. *J Virol* 83:1579–1591.
17. Rath S, Devey M (1988) IgG subclass composition of antibodies to HBsAg in circulating immune complexes from patients with hepatitis B virus infections. *Clin Exp Immunol* 72:164–167.
18. Prange R (2012) Host factors involved in hepatitis B virus maturation, assembly, and egress. *Med Microbiol Immunol* 201:449–461.
19. Ganem D, Schneider R (2001) Hepadnaviridae: The viruses and their replication. Philadelphia: Lippincott Williams & Wilkins, 4th edition, 2924 pp.
20. Glebe D, Urban S (2007) Viral and cellular determinants involved in hepadnaviral entry. *World J Gastroenterol* 13:22–38.
21. Ganem D (1991) Assembly of hepadnaviral virions and subviral particles. *Curr Top Microbiol Immunol* 168:61–83.
22. Gilbert R, Beales L, Blond D, Simon M, Lin B, et al. (2005) Hepatitis B small surface antigen particles are octahedral. *Proc Natl Acad Sci USA* 102:14783–14788.
23. Patient R, Hourieux C, Roingcard P (2009) Morphogenesis of hepatitis B virus and its subviral envelope particles. *Cell Microbiol* 11:1561–1570.
24. Garcia T, Li J, Sureau C, Ito K, Qin Y, et al. (2009) Drastic reduction in the production of subviral particles does not impair hepatitis B virus virion secretion. *J Virol* 83:11152–11165.
25. Nowak M, Bonhoeffer S, Hill A, Boehme R, Thomas H, et al. (1996) Viral dynamics in hepatitis B infection. *Proc Natl Acad Sci USA* 93:4398–4402.
26. Nowak M, May R (2000) *Virus Dynamics*. Oxford: Oxford University Press.
27. Perelson A (2002) Modelling viral and immune system dynamics. *Nature Rev Immunol* 2:28–36.
28. Perelson A, Neumann A, Markowitz M, Leonard J, Ho D (1996) HIV-1 dynamics in vivo: Virion clearance rate, infected cell life-span, and viral generation time. *Science* 271:1582–1586.
29. Stafford M, Corey L, Cap Y, Daar E, Ho D, et al. (2000) Modeling plasma virus concentration during primary HIV infection. *J Theor Biol* 203:285–301.
30. Lewin S, Ribeiro R, Walters T, Lau G, Bowden S, et al. (2001) Analysis of hepatitis B viral load decline under potent therapy: complex decay profiles observed. *Hepatology* 34:1012–1020.
31. Tsiang M, Rooney J, Toole J, Gibbs C (1999) Biphasic clearance kinetics of hepatitis B virus from patients during adefovir dipivoxil therapy. *Hepatology* 29:1863–1869.
32. Lambotte L, Saliez A, Triest S, Tagliaferri E, Barker A, et al. (1997) Control of rate and extent of the proliferative response after partial hepatectomy. *Am J Physiol* 273:G905–G912.
33. Michalopoulos G, DeFrances M (1997) Liver regeneration. *Science* 276:60–66.
34. Ciupe S, Ribeiro R, Nelson P, Perelson A (2007) Modeling the mechanisms of acute hepatitis B virus infection. *J Theor Biol* 247:23–35.
35. Bonhoeffer S, May R, Shaw G, Nowak M (1997) Virus dynamics and drug therapy. *Proc Natl Acad Sci USA* 94:6971–6976.
36. Ribeiro R, Dixit N, Perelson A (2006) Modelling the in vivo growth rate of HIV: implications for vaccination. *Multidisciplinary approaches to theory in medicine*. Amsterdam, Netherlands: Elsevier, 231–246 pp.
37. Nowak M, May R (2001) *Virus dynamics: Mathematical principles of immunology and virology*. Oxford University Press.
38. Murray J, Wieland S, Purcell R, Chisari F (2005) Dynamics of hepatitis B virus clearance in chimpanzees. *Proc Natl Acad Sci USA* 102:17780–17785.
39. Sprengers D, van der Molen R, Kusters J, De Man R, Niesters H, et al. (2006) Analysis of intrahepatic HBV-specific cytotoxic T-cells during and after acute HBV infection in humans. *J Hepatol* 45:182–189.
40. Yousfi N, Hattaf K, Tridane A (2011) Modeling the adaptive immune response in HBV infection. *J Math Biol* 63:933–957.
41. Kandathil A, Graw F, Quinn J, Hwang H, Torbenson M, et al. (2013) Use of laser capture microdissection to map hepatitis C virus-positive hepatocytes in human liver. *Gastroenterol* 145:1404–1413.
42. Dibrov B, Lívshits M, Volkenstein M (1977) Mathematical model of immune processes. *J Theor Biol* 65:609–631.
43. Oprea M, Perelson A (1996) Exploring the mechanisms of primary antibody responses to T cell-dependent antigens. *J Theor Biol* 181:215–236.
44. Lodish H, Berk A, Matsudaira P, Kaiser C, Krieger M, et al. (2004) *Molecular Cell Biology*. San Francisco, CA: WH Freeman & Co, 5th edition.
45. Sherlock S, Dooley J (2002) *Diseases of the Liver and Biliary System*. Oxford: Blackwell Science, 11 edition, 1–9 pp.
46. Dahari H, Cotler S, Layden T, Perelson A (2009) Hepatitis B virus clearance rate estimates. *Hepatology* 49:1779–1780.
47. Dati F, Schumann G, Thomas L, Aguzzi F, Baudner S, et al. (1996) Consensus of a group of professional societies and diagnostic companies on guidelines for interim reference ranges for 14 proteins in serum based on the standardization against the IFCC/BCR/CAP reference material (CRM 470). *Eur J Clin Chem Clin Biochem* 34:517–520.
48. Gonzalez-Quintela A, Alende R, Gude F, Campos J, Rey J, et al. (2007) Serum levels of immunoglobulins (IgG, IgA, IgM) in a general adult population and their relationship with alcohol consumption, smoking and common metabolic abnormalities. *Clin Exp Immunol* 151:42–50.
49. Morell A, Terry W, Waldmann T (1970) Metabolic properties of IgG subclasses in man. *J Clin Invest* 49:673–680.
50. Rossi M, Azzari C, Resti M, Appendino C, Pezzati P, et al. (1988) Selectivity in IgG subclass response to hepatitis B vaccine in infants born to HBsAg-positive mothers. *Clin Exp Immunol* 72:196–200.
51. Rath S, Devey M (1988) IgG subclass composition of antibodies to HBsAg in circulating immune complexes from patients with hepatitis B virus infections. *Clin Exp Immunol* 72:164–167.
52. Schwesinger F, Ros R, Strunz T, Anselmetti D, Guntherodt HJ, et al. (2000) Unbinding forces of single antibody-antigen complexes correlate with their thermal dissociation rates. *Proc Natl Acad Sci USA* 97:9972–9977.
53. Gopalakrishnan P, Karush F (1975) Antibody affinity. VIII. measurement of affinity of anti-lactose antibody by fluorescence quenching with a DNP-containing ligand. *J Immunol* 114:1359–1362.
54. Roost H, Bachmann M, Haag A, Kalinke U, Pliska V, et al. (1995) Early high-affinity neutralizing anti-viral IgG responses without further overall improvements of affinity. *Proc Natl Acad Sci USA* 92:1257–1261.
55. Igarashi T, Brown C, Azadegan A, Haigwood N, Dimitrov D, et al. (1999) Human immunodeficiency virus type 1 neutralizing antibodies accelerate clearance of cell-free virions from blood plasma. *Nat Med* 5:211–216.
56. Webster G, Hallett R, Whalley S, Meltzer M, Balogun K, et al. (2000) Molecular epidemiology of a large outbreak of hepatitis B linked to autohaemotherapy. *Lancet* 356:379–384.
57. Whalley S, Murray J, Brown D, Webster G, Emery V, et al. (2001) Kinetics of acute hepatitis B virus infection in humans. *J Exp Med* 193:847–853.
58. Klasse P, Sattentau Q (2002) Occupancy and mechanism in antibody-mediated neutralization of animal viruses. *J Gen Virol* 83:2091–2108.
59. Yang X, Lee SKS, Sodroski J (2005) Stoichiometry of antibody neutralization of human immunodeficiency virus type 1. *J Virol* 79:3500–3508.
60. Magnus C, Regoes R (2011) Restricted occupancy models for neutralization of HIV virions and populations. *J Theor Biol* 283:192–202.
61. Magnus C (2013) Virus neutralisation: New insights from kinetic neutralisation curves. *PLoS Comput Biol* 9:e1002900. doi:10.1371/journal.pcbi.1002900.
62. IgG Human ELISA Kit ab100547 <http://www.abcam.com/IgG-Human-ELISA-Kit-ab100547.html>.
63. Bortz D, Nelson P (2004) Sensitivity analysis of a nonlinear lumped parameter model of HIV infection dynamics. *Bull Math Biol* 66:1009–1026.
64. Tabei A, Li Y, Weigert M, Dinner A (2012) Model for competition from self during passive immunization, with application to broadly neutralizing antibodies for HIV. *Vaccine* 30:607–613.
65. Tomaras G, Yates N, Liu P, Qin L, Fouda G, et al. (2008) Initial B-cell responses to transmitted human immunodeficiency virus type 1: virion-binding immunoglobulin IgM and IgG antibodies followed by plasma anti-gp41 antibodies with ineffective control of initial viremia. *J Virol* 82:12449–12463.
66. Hadler S, Margolis H (1992) Hepatitis B immunization: vaccine types, efficacy, and indications for immunization. *Curr Clin Top Infect Dis* 12:282–308.
67. McMahon B, Bruden D, Petersen K, Bulkow L, Parkinson A, et al. (2005) Antibody levels and protection after hepatitis B vaccination: results of a 15-year follow-up. *Ann Intern Med* 142:333–341.
68. McMahon B, Dentinger C, Bruden D, Zanis C, Peters H, et al. (2009) Antibody levels and protection after hepatitis B vaccine: Results of a 22-year follow-up study and response to a booster dose. *J Inf Dis* 200:1390–1396.
69. Cejka J, Mood D, Kim C (1974) Immunoglobulin concentrations in sera of normal children: quantitation against an international reference preparation. *Clin Chem* 20:656–659.
70. Parkin D (2006) The global health burden of infection-associated cancers in the year 2002. *Int J Cancer* 118:3030–3044.
71. Read S (2001) Recovery efficiencies of nucleic acid extraction kits as measured by quantitative LightCycler TM PCR. *Mol Path* 54:86–90.